



# Research of Frequency Coordinated Control Strategy Based on Variable De-loading Level for D-PMSG Wind Turbine

Mudan Li<sup>1,2</sup> · Yinsong Wang<sup>1,2</sup>

Received: 23 June 2020 / Revised: 19 August 2020 / Accepted: 18 September 2020 / Published online: 9 October 2020  
© The Korean Institute of Electrical Engineers 2020

## Abstract

A new frequency coordinated control strategy based on the variable de-loading level for a D-PMSG wind turbine is proposed. First, the D-PMSG wind turbine model and control system model are established. Second, the de-loading control principle of the D-PMSG wind turbine is described, the variable de-loading level control strategy is analyzed according to different wind speeds and additional inertial control is introduced. Then the frequency coordinated control strategy combining variable de-loading level control and additional inertial control is designed for different power reserve areas. Finally, a D-PMSG grid-connected simulation system is built to verify the rationality and accuracy of the frequency coordinated control strategy.

**Keywords** D-PMSG · Wind turbine · Frequency modulation · Variable de-loading level control · Coordinated control

## 1 Introduction

As a clean energy source with substantial development prospects, wind energy has been globally recognized as the best solution for improving energy security and promoting low-carbon economic growth [1, 2]. However, due to the uncertainty of wind speed, wind power is random and intermittent, and large-scale grid-connected wind power will affect the power system frequency stability and increase the difficulty of frequency control [3, 4]. To enhance the ability of the grid to accept wind power, it is important to heighten the wind power frequency modulation and control capabilities.

Directly driven wind turbines with permanent magnet synchronous generators (D-PMSGs) without troublesome gearboxes have attracted considerable attention due to their high efficiency, high reliability, competitive cost and wide operating ranges [5–7]. In the maximum power point tracking (MPPT) control mode, the D-PMSG hardly contributes to the system inertia and shows weak support for the frequency stability owing to the decoupling of the rotor speed and system frequency. Large-scale grid-connected wind

power inevitably causes a lower system inertia and an insufficient frequency modulation ability [8–10]. Therefore, it is of great theoretical and practical significance to study the D-PMSG frequency control strategy for participation in the grid frequency modulation.

To improve the frequency modulation capability and strategy for grid-connected wind power, scholars worldwide have performed many studies. Based on the system frequency variation, the inertial response of synchronous generators can be simulated, and the wind turbine rotor speed or pitch angle can be adjusted to generate additional output power for system frequency modulation. For the rapid frequency change caused by the load disturbance in the power system, inertial control can achieve a better frequency modulation effect. However, the settling time is short, and the grid frequency would drop again when the rotor speed recovers. In [11–14], a frequency response control link is added to the rotor side to adjust the active power and system frequency. In [15–17], an additional inertial control module is added to the wind turbine to simulate the inertial response of synchronous generators and to achieve fast active power regulation. However, due to the mutual influence between the inertia response and the MPPT control, it is not conducive for wind turbines to provide power support to the system. De-loading control is another method for frequency modulation that includes two types: over-speed control and pitch angle control. In [18, 19], the doubly-fed wind turbine rotor speed is adjusted to exceed the optimal value to obtain the reserved power and

✉ Mudan Li  
limudan6017291@163.com

<sup>1</sup> Science and Technology College, North China Electric Power University, Baoding, China

<sup>2</sup> College of Control and Computer Engineering, North China Electric Power University, Baoding, China

achieve de-loading operation. However, due to the restriction of the rated rotor speed, over-speed control only applies to low and medium wind speed zones. In [20, 21], a pitch angle control method is introduced for de-loading in the high wind speed zone, and the pitch angle is adjusted in a timely manner to regulate the active power once the system frequency deviated. However, frequently changing the pitch angle will shorten the operating life of the wind turbine. Multiple power reserve control schemes are compared in [22, 23]. The power reserve control effect is optimal when over-speed-pitch cooperative control is applied in the low wind speed zone and pitch angle control is adopted in the high wind speed zone. In [24, 25], low, medium and high wind speed zones are determined based on the wind speed, a power reserve control strategy with a fixed de-loading level is adopted and different power reserve themes are employed for different zones to control the wind turbine output power. In [26], a power reserve control strategy that combines a fixed de-loading level and constant power is utilized to participate in system frequency modulation, and improve the economic efficiency of grid-connected wind turbines. However, the de-loading control strategy with a fixed de-loading level may provide different reserved power levels in different wind speed zones, which fails to provide the expected active power and exit the power reserve control under low wind speeds. Otherwise, the redundancy of the reserved power under high wind speeds will reduce the economy of operation.

Many studies have proposed combining these two methods. In [27–29], de-loading control and inertia control in different wind speed zones for doubly fed induction generators (DFIGs) are integrated to participate in system frequency modulation. Over-speed control and inertia control are combined when the wind speed is less than the rated value. Otherwise, pitch angle control and inertia control are combined to provide fast and stable active power. Different frequency control methods are adopted in [30] to participate in the primary frequency regulation in full wind conditions. An inertial control strategy is employed when the wind speed is low; pitch angle control is utilized when the wind speed continues to increase; and an over-loading control strategy is adopted when the wind speed is high. In [31], the over-speed control and pitch angle control strategies are combined to participate in frequency modulation. However, the fast power support of inertial control is disregarded.

Although these studies improve the frequency modulation capability of a grid-connected wind power system to some extent, none of them adequately combined the inertial control strategy and de-loading control strategy in the full wind speed zones, and did not consider the defects of a fixed de-loading level. Therefore, a frequency coordinated control strategy that combines a variable de-loading level control and inertial control is proposed in this paper to take full advantage of the

rapidity of inertial control and the continuity of de-loading control for frequency modulation, overcome the shortcomings of a fixed de-loading level and further improve the D-PMSG frequency modulation capability in the full wind speed zones.

The main contributions of this paper may be summarized as follows:

1. A D-PMSG grid-connected system is presented and a simplified D-PMSG model that considers power–frequency characteristics is established.
2. The variable de-loading level under different wind speeds is defined and a variable de-loading level control strategy is proposed based on the principle of de-loading control, and an additional inertial control strategy is introduced and discussed.
3. The low, medium and high wind speed zones are divided, different frequency coordinated control strategies for different zones are designed and the principles are illustrated.
4. The rationality and accuracy of the proposed frequency coordinated control strategy compared with MPPT control, de-loading control and additional inertial control strategies for D-PMSG wind turbines are verified by simulation under sudden load changes.

The remainder of this paper is arranged as follows. The D-PMSG wind turbine model and control systems are introduced in Sect. 2. The D-PMSG variable de-loading level control in full wind speed zones is presented in Sect. 3. The D-PMSG frequency coordinated control strategy is designed in Sect. 4. The effectiveness of the proposed frequency coordinated control strategy is assessed by means of the MATLAB/Simulink platform in Sect. 5. Some conclusions are presented in Sect. 6.

## 2 D-PMSG Wind Turbine Model and Control System Model

A typical structure of the D-PMSG grid-connected system [32] is mainly comprised of a simplified model of the D-PMSG, converter, transformer, and equivalent synchronous generator set (ESGS), as shown in Fig. 1. The ESGS is a simulation of the grid.

According to the aerodynamic principle, the actual output mechanical power of the wind turbine can be stated as (1) [33].

$$\begin{cases} P_w = C_p(\lambda, \beta)P_{\text{wind}} = \frac{1}{2}\rho\pi R^2 v^3 C_p(\lambda, \beta) \\ C_p(\lambda, \beta) = (0.44 - 0.0167\beta)\sin\left[\frac{\pi(\lambda - 3)}{15 - 0.3\beta}\right] - 0.00184(\lambda - 3)\beta \\ \lambda = \omega_r R / v \end{cases} \quad (1)$$

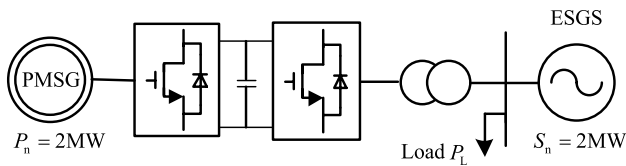


Fig. 1 Typical structure of D-PMSG grid-connected system

where  $\rho$  is the air density ( $\text{kg/m}^3$ ),  $C_p(\lambda, \beta)$  is the power coefficient with a theoretical optimal value of 0.593,  $\lambda$  is the tip speed ratio,  $\beta$  is the blade pitch angle ( $^\circ$ ),  $R$  is the wind turbine blade radius (m) and  $\omega_r$  is the wind turbine rotor speed (rad/s).

Disregarding the flexible shaft and the mechanical loss between the wind turbine rotor and generator, an equivalent single mass model is adopted to simulate the transmission device [33, 34]:

$$\frac{d\omega_r}{dt} = \frac{1}{H_w}(T_m - T_e) \tag{2}$$

where  $H_w$  is the inertia time constant of the equivalent single mass model,  $T_m$  is the wind turbine mechanical torque, and  $T_e$  is the electromagnetic torque.

The frequency response characteristics of the power system are electro-mechanical transient processes that are mainly affected by the D-PMSG power–frequency characteristics. Considering the active output characteristics [35, 36], the PMSG and converter are equivalent to an inertia link in this paper. The simplified mathematical model of the PMSG and converter can be stated as

$$P_e = \frac{1}{1 + sT_A} P_{opt} \tag{3}$$

where  $P_e$  is the output active power of the wind turbine,  $P_{opt}$  is the reference signal of the PMSG active power, and  $T_A$  is the equivalent time constant of the PMSG and converter.

The operating range of the D-PMSG is generally divided into two areas based on different wind speed zones. When the wind speed is lower than the rated value, the pitch angle is zero, and the optimal tip speed ratio is maintained by adjusting the rotor speed to implement MPPT control. When the wind speed is higher than the rated value, the rotor speed and output power have reached the limit value, and pitch angle control should be introduced to maintain the invariable output power.

According to the MPPT control principle, the active power reference signal  $P_{opt}$  can be determined by (4) [37].

$$P_{opt} = 0.5\rho\pi R^2 v^3 C_{P_{max}}(\lambda, \beta) \tag{4}$$

where  $C_{P_{max}}$  is the maximum power coefficient.

The blade pitch angle is adjusted via the pitch angle control section to regulate the active output power of the wind turbine. The pitch angle remains  $0^\circ$  when the wind speed is lower than the rated value; in contrast, the pitch angle is adjusted to maintain the rated output power.

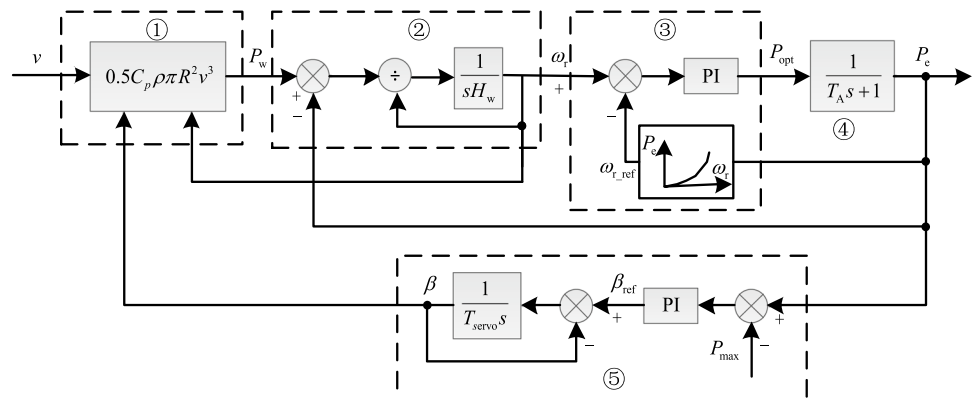
The simplified model of the D-PMSG wind turbine is shown in Fig. 2, in which ①, ②, ③, ④, and ⑤ are the wind turbine model, transmission mechanism model, MPPT control system model, PMSG/converter model and pitch angle control system model, respectively.

### 3 Principle of Variable De-loading Level Control for the D-PMSG Wind Turbine

#### 3.1 A. Principle of de-loading control for the D-PMSG wind turbine

Variable speed wind turbines usually operate in the MPPT control mode to maximize the wind energy utilization and cannot provide additional active power to participate in frequency modulation, which reduces the stability of the power system operation. Therefore, the D-PMSG wind turbine needs to perform a de-loading operation to provide reserved

Fig. 2 Simplified model of D-PMSG wind turbine



power and participate in frequency modulation when the system frequency changes.

At a certain wind speed with a  $d\%$  de-loading level, the reserved active power for a D-PMSG wind turbine is stated as:

$$\begin{aligned} \Delta P_G &= d\% \cdot P_{opt} = d\% \cdot 0.5\rho\pi R^2 v^3 C_{Pmax}(\lambda, \beta) \\ &= 0.5\rho\pi R^2 v^3 \cdot d\% C_{Pmax}(\lambda, \beta) \end{aligned} \tag{5}$$

where  $\Delta P_G$  is the reserved power at the  $d\%$  de-loading level, and  $P_{opt}$  is the maximum power reference value. It can be seen that the D-PMSG wind turbine can operate in the de-loading mode with a power coefficient that decreases by  $d\%$  while maintaining the constant wind speed  $v$  and air density  $\rho$ .

As shown in Fig. 3, A is the optimal output power at  $v_0$  with the optimal rotor speed  $\omega_{r0}$  and initial pitch angle  $\beta_0$ . The power coefficient can be reduced by  $d\%$  by means of increasing  $\omega_{r0}$  to  $\omega_{r1}$  or increasing  $\beta_0$  to  $\beta_1$ . These are the over-speed control and pitch angle control that can realize the de-loading operation and provide reserved active power for the D-PMSG frequency modulation.

### 3.2 B. Principle of Variable De-loading Level Control for the D-PMSG Wind Turbine

Due to the differences in the meteorological conditions and aerodynamic uncertainties, the operating conditions of each wind turbine in a wind farm are different. When participating in frequency modulation, a fixed de-loading level for the D-PMSG wind turbine may generate insufficient reserved power and exit the frequency modulation under low wind speeds. Otherwise, the reserved power may be redundant, which will reduce the turbine operation economy when the wind speed is high.

The idea of variable de-loading level control is proposed in this paper, and different de-loading levels are

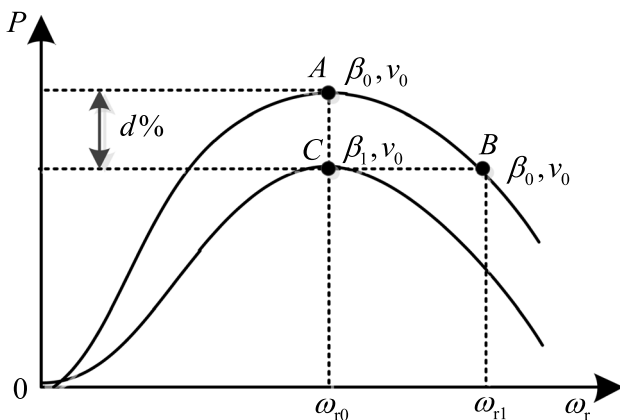


Fig. 3 Principle diagram of de-loading control

adopted to implement power reserve control under different wind speeds. The variable de-loading level is defined as

$$d\% = \frac{\Delta P_G}{P_{opt}} = \frac{\Delta f}{\sigma_\omega \cdot P_{opt}} \tag{6}$$

where  $\Delta P_G$  is the reserved power, which is determined by the system frequency deviation  $\Delta f$  and static droop value  $\sigma_\omega$ .

Generally, the D-PMSG optimal output power differs at different wind speeds. According to Eq. (6), to obtain a fixed reserved power at different wind speeds, the de-loading levels also differ when  $\Delta f$  and  $\sigma_\omega$  are given. The relationship between the wind turbine output power and the rotor speed under variable de-loading level control is indicated in Fig. 4. Three different power reserve control areas are divided according to different wind speeds.

- (1) Over-speed power reserve area. The wind speed is  $v \in [v_{in}, v_1]$ , and the D-PMSG reserved power is achieved by over-speed control. As shown in Fig. 4,  $A'$  is the over-speed operation point of A, where the reserved power is stated as

$$\Delta P_{Ga} = d\%_a \cdot P_{optA} \tag{7}$$

where  $d\%_a$  is the de-loading level when  $v = v_{in}$ .

- (2) Over-speed-pitch power reserve area. When the wind speed is  $v \in [v_1, v_n]$ , the D-PMSG expected reserved power cannot be obtained due to the limitation of the maximum rotor speed and the output power can be reduced by adjusting the pitch angle. As shown in Fig. 4,  $E'$  is the over-speed-pitch operation point of E, where the reserved power is stated as

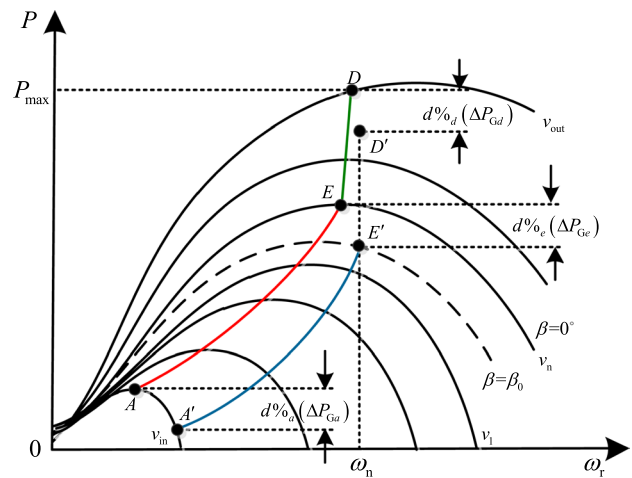


Fig. 4 Relationship between the wind turbine output power and the rotor speed

$$\Delta P_{Ge} = d\%_e \cdot P_{optE} \tag{8}$$

where  $d\%_e$  is the de-loading level when  $v = v_n$ .

- (3) Pitch angle power reserve area. When the wind speed is  $v \in [v_n, v_{out}]$ , the over-speed control cannot be implemented, and the reserved power can only be achieved by adjusting the pitch angle. As shown in Fig. 4,  $D'$  is the pitch angle operation point of  $D$ , where the reserved power is stated as

$$\Delta P_{Gd} = d\%_d \cdot P_{optD} \tag{9}$$

where  $d\%_d$  is the de-loading level when  $v=v_{out}$ .

It can be seen that the D-PMSG can obtain a definite reserved power that adopts a variable de-loading level control strategy for different wind speeds, which can ensure that the wind turbine effectively participates in frequency modulation when the wind speed is low, provides appropriate reserved power when the wind speed is high, and improves the D-PMSG operation economy.

### 3.3 C. Principle Of Additional Inertial Control For The D-Pmsg Wind Turbine

The D-PMSG wind turbine is usually connected to the power grid via a full power converter. Due to the decoupling of the rotor speed and system frequency, the rotor speed cannot be adjusted to regulate the active power according to the system frequency deviation. The additional inertial control strategy introduces the proportional and derivative terms of the system frequency deviation to generate an additional active power that is proportional to the frequency deviation and differentiation for rapid active power adjustment when the system frequency fluctuates. The additional active power is stated as:

$$\Delta P_f = \Delta P_{f1} + \Delta P_{f2} = -k_p \Delta f - k_d \frac{d\Delta f}{dt} \tag{10}$$

where  $\Delta P_f$  is the additional active power,  $\Delta P_{f1}$  is proportional to the frequency deviation, which is the additional power of droop control;  $\Delta P_{f2}$  is proportional to the frequency differentiation, which is the additional power of inertial control; and  $k_p, k_d$  are the droop control coefficient and the inertial control coefficient, respectively.

The additional power of inertial control can quickly increase or decrease the electromagnetic power during the early stage of a frequency change and ensure fast frequency modulation. The additional power of droop control can be converted to an additional de-loading level at the corresponding wind speed, and the wind turbine output power can be changed by adjusting the de-loading level. According

to Eq. (6), the additional de-loading level can be described as follows:

$$d\%_f = \frac{\Delta P_{f1}}{\sigma_\omega} = -\frac{k_p}{\sigma_\omega} \Delta f \tag{11}$$

Therefore, the D-PMSG new de-loading level can be stated as:

$$d\%_{ref} = d\% + d\%_f \tag{12}$$

Thus, the initial de-loading level can be replaced to adjust the D-PMSG output power and implement frequency modulation.

## 4 D-PMSG Frequency Coordinated Control Strategy Based on Variable De-loading Level Control

### 4.1 A. Division of the Wind Speed Zones

Three wind speed zones are divided for the D-PMSG wind turbine to accurately switch to the corresponding power reserve control area when the wind speed changes. As shown in Fig. 5, the solid red line indicates the MPPT curve; the solid blue line indicates the de-loading curve at the  $d\%$  de-loading level; and the dotted green line represents the pitch angle curve.

The low wind speed Zone 1 is  $v_{cut-in} \sim v_1$ , the medium wind speed Zone 2 is  $v_1 \sim v_n$ , and the high wind speed Zone 3 is  $v_n \sim v_{cut-out}$ , where  $v_{cut-in}, v_n$  and  $v_{cut-out}$  are the cut-in wind speed, rated wind speed and cut-out wind speed of the D-PMSG, respectively.  $v_1$  is the wind speed limit to ensure a certain reserved power only by over-speed control.

The power coefficient  $C_{Pv}$  at the certain wind speed  $v$  can be obtained by Eq. (13):

$$\begin{cases} C_{Pv}(\lambda, \beta) = (1 - \Delta P_G / P_{opt}) \cdot C_{Pmax} \\ C_{Pv}(\lambda, \beta) = C_{Pv}(\lambda_n, 0) \\ \lambda_n = \omega_n R / v \end{cases} \tag{13}$$

where  $\Delta P_G$  is the reserved power.  $v_1$  can be acquired by

$$v_1 = \frac{\omega_n \cdot R}{\lambda_n} \tag{14}$$

If  $v < v_1$ , then the required reserved power can be achieved only by over-speed control. If  $v_1 < v < v_n$ , then it is necessary to combine the pitch angle control for the de-loading operation. If  $v > v_n$ , then the D-PMSG rotor speed and output power have reached the rated value, and the pitch angle needs to be adjusted to implement de-loading.

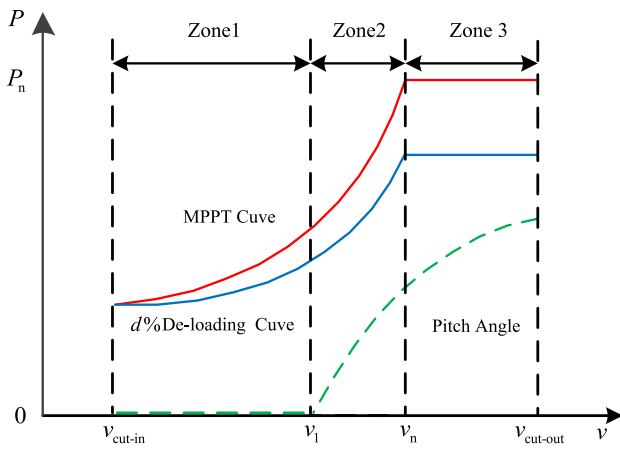


Fig. 5 Division of wind speed zones

### 4.2 B. Principle of the Frequency Coordinated Control Strategy in Different Power Reserve Areas

A frequency coordinated control strategy is proposed in this paper to improve the frequency modulation capability for the D-PMSG wind turbines. Variable de-loading level control is adopted to achieve reserved power. On the other hand, additional inertial control is introduced to provide rapid power support. Three frequency modulation areas are divided according to the power reserve characteristics in different wind speed zones.

(1) Frequency modulation principle in the over-speed power reserve area

The D-PMSG reserved power is achieved only by over-speed control if  $v < v_1$ . The principle of the frequency

coordinated control strategy is shown in Fig. 6. First, the system initial de-loading level  $d\%$  is calculated according to  $\Delta f$ ,  $\sigma_\omega$  and  $P_{opt}$  based on Eq. (6). When the system frequency changes, the additional power of inertial control  $\Delta P_{f2}$  is added to the input reference power of the machine-side converter via the speed protection module (SPM) to obtain fast inertial support. The SPM is employed to protect the rotor speed in a proper range. In addition, the additional power of droop control is converted to an additional de-loading level  $d\%_f$  based on Eq. (11), which is superimposed on the initial level to generate the new de-loading level  $d\%_{ref}$ . If  $d\%_{ref} > 0$ , then the initial level is substituted, and the output power is increased to implement frequency modulation. If  $d\%_{ref} \leq 0$ , then the wind turbine operates in the MPPT control mode and releases all the reserved power.

(2) Frequency modulation principle in the over-speed-pitch power reserve area

The D-PMSG rotor speed has reached the rated value when  $v_1 < v < v_n$ , and pitch angle control is necessary for a power reserve. The corresponding frequency coordinated control strategy principle is shown in Fig. 7.

The D-PMSG initial de-loading level  $d\%$  at the wind speed  $v$  is determined. When the system frequency changes, inertial control is adopted to provide fast power support. On the other hand, the pitch angle is adjusted in response to the frequency deviation. As shown in Fig. 7,  $\beta_0$  is the initial pitch angle required for the de-loading operation which is defined based on Eq. (15)

$$\begin{cases} C_{Pv}(\lambda, \beta) = C_{Pv}(\lambda_n, 0) = (1 - d\%) C_{Pmax} \\ \lambda_n = \omega_n R / v \end{cases} \quad (15)$$

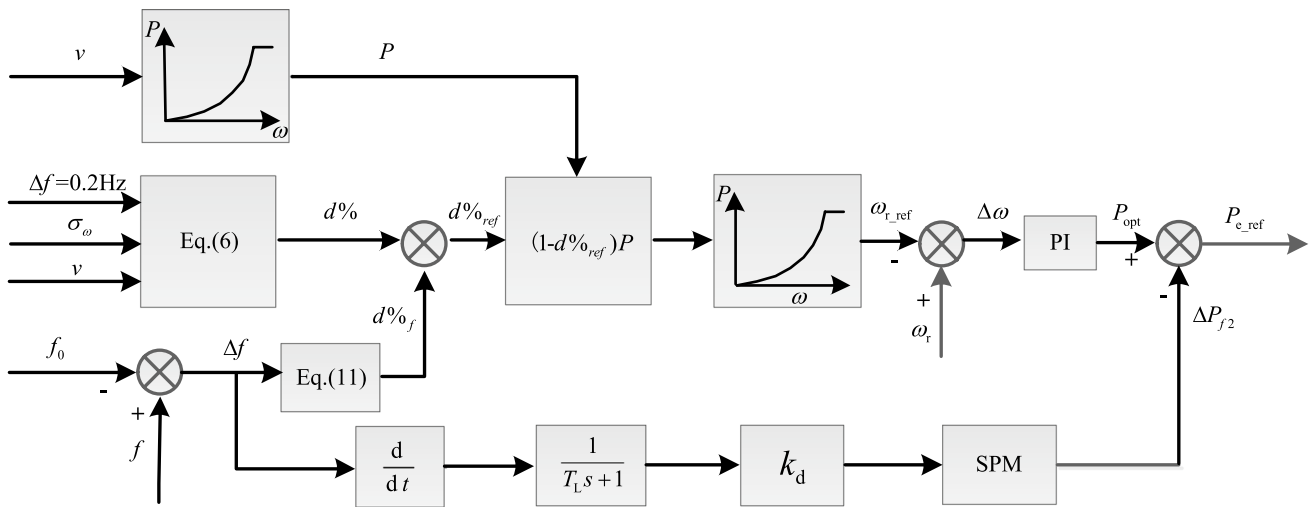


Fig. 6 Structure diagram of frequency coordinated control in over-speed power reserve area

Because of the serious nonlinearity in  $C_p(\lambda, \beta)$ , directly solving the initial pitch angle  $\beta_0$  is difficult. Therefore, the Simulink simulation method is used with the sampling interval  $\Delta v$  when  $v_1 < v < v_n$ . Thus, the wind speed and initial pitch angle data pair  $\{v(i), \beta_0(i)\}, i = 1, 2, \dots, (v_n - v_1)/\Delta v$  can be obtained. Based on the least squares method,  $\beta_0$  is stated as follows:

$$\beta_0 = f(v) = \varepsilon_0 + \varepsilon_1 v + \varepsilon_2 v^2 + \dots + \varepsilon_n v^n \quad (16)$$

As shown in Fig. 7, the D-PMSG pitch angle required for frequency modulation is described as:

$$\beta = \beta_0 + \Delta\beta \quad (17)$$

where  $\Delta\beta$  is the pitch angle increment, which is calculated by the following equation:

$$\Delta\beta = k_\beta \Delta f \quad (18)$$

where  $k_\beta$  is the adjustment coefficient of the pitch angle,  $-\Delta f_1 < \Delta f < \Delta f_1$ , and  $\pm\Delta f_1$  represents the frequency deviation limits.

(3) Frequency modulation principle in the pitch angle power reserve area

The D-PMSG rotor speed and output power have reached the rated value when  $v > v_n$ , and it is necessary to introduce pitch angle control to achieve reserved power during wind speed changes. However, the continuation of inertial control will result in a rapid power increase and decrease the rotor speed and output power. Therefore, only de-loading control is required to participate in the frequency modulation in the pitch angle power reserve area. The principle of frequency modulation is shown in Fig. 8.

First, the D-PMSG initial de-loading level  $d\%$  is determined by the rated power  $P_n$  and the required reserved

power  $\Delta P_G$ . The additional de-loading level  $d\%_f$  obtained by the droop control is superimposed on the initial de-loading level to generate the new value  $d\%_{ref}$ . Thus, the de-loading level can be changed to adjust the pitch angle.

## 5 Simulation Analysis

### 5.1 A. Brief Introduction of the Simulation System

A simulation system, as shown in Fig. 1, is built based on the MATLAB/Simulink platform. Figure 9 illustrates the structure diagram of the ESGS, which is composed of a speed control system, a turbine and a synchronous generator, where the speed control system consists of a governor and a servo mechanism [38]. Partial parameters have been marked, and the remaining values of the simulation system are summarized in the Appendixes.

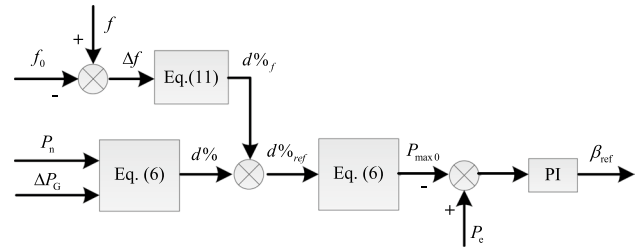
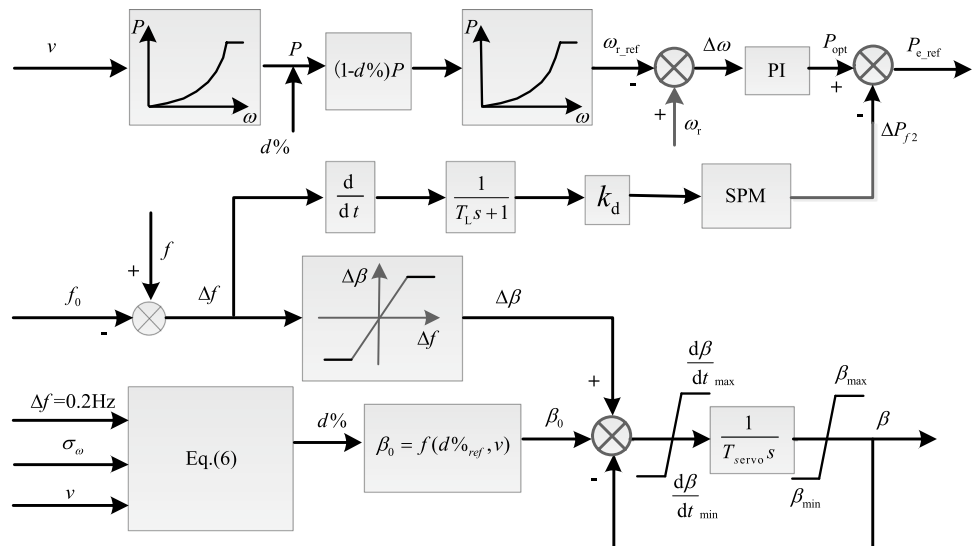


Fig. 8 Structure diagram of frequency control in the pitch angle power reserve area

Fig. 7 Structure diagram of frequency coordinated control in the over-speed-pitch power reserve area



### 5.2 B. Relationship Between The Wind Speed And The De-Loading Level

In the proposed frequency coordinated control strategy with a variable de-loading level, different de-loading levels are utilized to guarantee a certain reserved power at different wind speeds. When the system installed capacity is relatively large, setting the system frequency deviation to  $\Delta f = \pm 0.02$  Hz and the optimal power to different wind speeds is definite for a determined type of D-PMSG. Based on the range of the static droop value for the thermal power turbine (2–5%), the value of the D-PMSG is set to  $\sigma_\omega = 4\%$ . According to Eq. (5), the reserved power at different wind speeds is  $\Delta P_G = 0.1$  p.u., and the corresponding de-loading level can be determined by Eq. (6). For a GW82/1500 D-PMSG wind turbine with the cut-in wind speed  $v_{in} = 3$  m/s and rated wind speed  $v_n = 10.3$  m/s, the de-loading level at different wind speeds is indicated in Fig. 10.

The D-PMSG de-loading level differs at different wind speeds. Furthermore, the de-loading level decreases with an increase in wind speed, especially the de-loading level is  $d\% = 10\%$  when the wind speed reaches 8.5 m/s.

### 5.3 C. Relationship Between the Wind Speed and Initial Pitch Angle in Medium Wind Speed Zone 2

The wind speed limit is  $v_1 = 8.94$  m/s based on the previous discussion. Taking the sampling interval as  $\Delta v = 0.1$  m/s when  $v \in [8.94, 10.3]$  m/s, 14 data pairs of  $\{v(i), \beta_0(i)\}, i = 1, 2, \dots, 14$  are obtained via the Simulink simulation, as shown in Table 1.

The fitted initial pitch angle  $\beta_0$  is expressed as follows:

$$\beta_0 = 0.0287v^3 - 1.2046v^2 + 15.506v - 60.68 \quad (19)$$

It can be seen that the initial pitch angle and wind speed show a strong nonlinearity. However, the variation range of the initial pitch angle is relatively small.

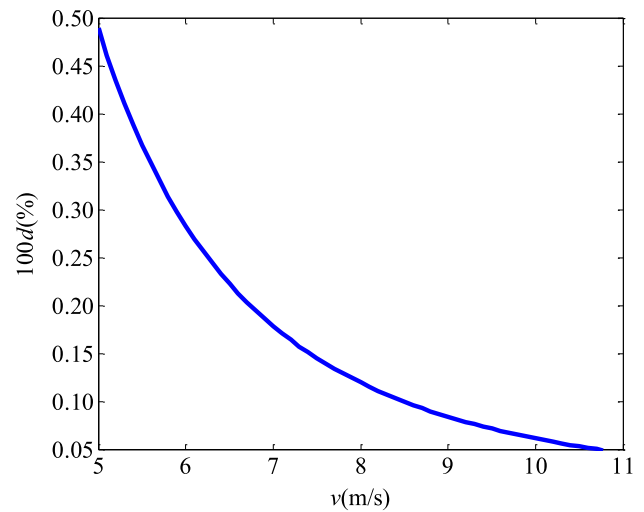


Fig. 10 De-loading level at different wind speeds

## 6 D. Simulation Analysis Under a Sudden Load Change

Comprehensive MATLAB/Simulink simulations have been carried out to verify the superiorities of the proposed frequency coordinated control strategy with variable de-loading levels in the three power reserve areas. Three representative wind speeds (8 m/s, 10 m/s and 12 m/s) were chosen to perform simulations and analysis under sudden load changes.

- (1) Simulation analysis in the over-speed power reserve area.

The wind speed is set to 8 m/s and the de-loading level is 11.9% under variable de-loading level control. In the first 5 s, the active power of the load increases by 0.4 MW, and other relevant parameters are selected as  $T_L = 0.1$  s,  $k_p = 0.3$  and  $k_d = 0.4$ . Simulation tests are carried out by adopting four control strategies: (1) MPPT control; (2) additional inertial control; (3) variable de-loading level control; (4) frequency coordinated control. The simulation results are shown in Fig. 11.

Figure 11(a) illustrates the comparisons of the system frequency response after the load suddenly increases. Partial data are shown in Table 2.

Fig. 9 Structure diagram of the ESGS

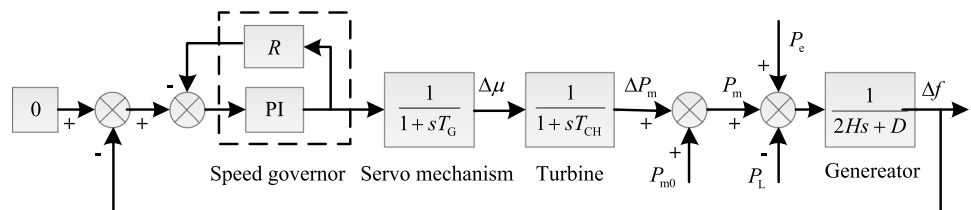




**Table 1** Data pairs of  $\beta_0$  and  $v$

$v/(m/s)$	9	9.1	9.2	9.3	9.4	9.5	9.6
$\beta_0/^\circ$	2.22	2.29	2.37	2.42	2.47	2.51	2.54
$v/(m/s)$	9.7	9.8	9.9	10	10.1	10.2	10.3
$\beta_0/^\circ$	2.56	2.57	2.59	2.61	2.63	2.62	2.58

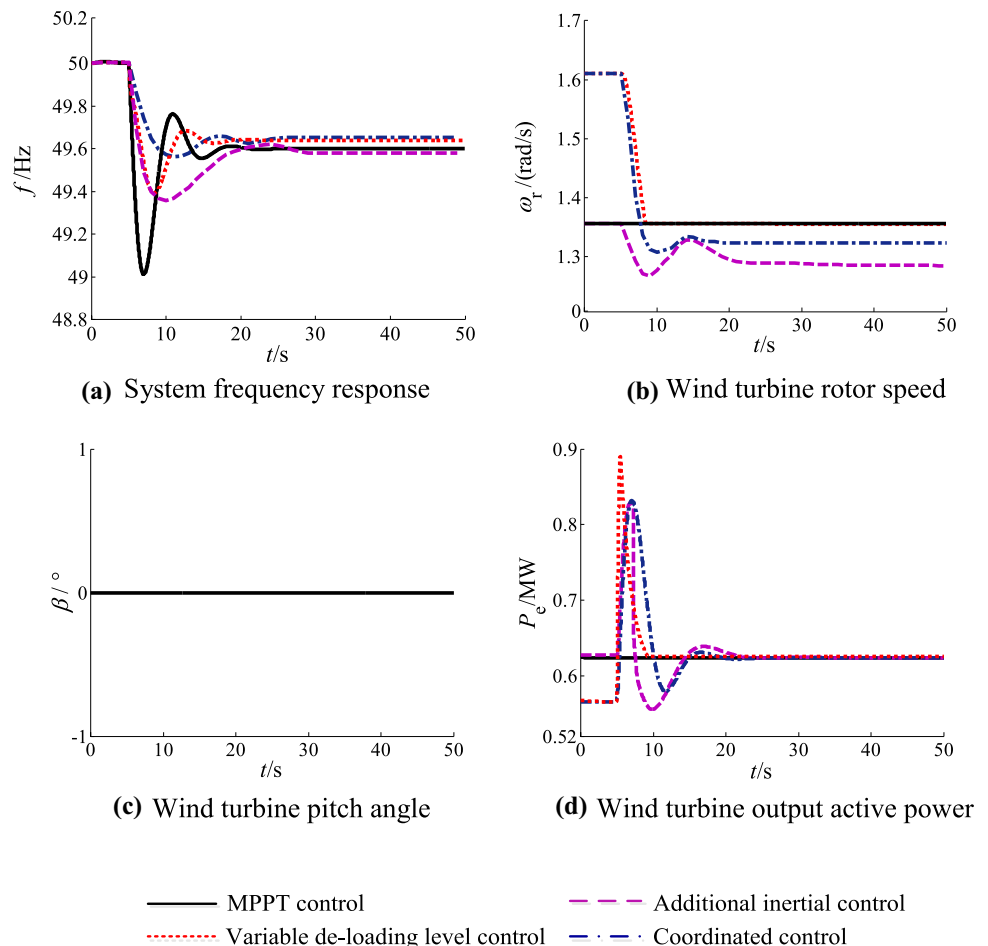
Note: AIC control: additional inertial control; VD-L control: variable de-loading level control; CO control: coordinated control;  $f_{min}$ ,  $t_{min}$ ,  $f_\infty$ ,  $t_\infty$  are the system frequency minimum value, time to system frequency minimum value, system frequency steady-state value, and system frequency setting time, respectively.

Obviously, when the system frequency changes, the D-PMSG rotor speed, pitch angle and output power remain constant due to decoupling of the rotor speed and the system frequency in the MPPT control mode. In the additional inertial control mode, the system frequency change rate decreases, the minimum value increases from 49.01 Hz to 49.37 Hz and the time to system frequency minimum value extends from 7.0 s to 10.7 s. However, the system frequency steady-state response is hardly improved. In the case of variable de-loading level control,

the system frequency variation is significantly reduced due to the faster response of over-speed control, the system frequency minimum value increases to 49.42 Hz and the steady-state value increases from 49.60 Hz to 49.62 Hz. In the case of frequency coordinated control, the system frequency minimum value is further increased to 49.59 Hz, the time to the minimum value is prolonged to 12.6 s, and the frequency steady state value is raised to 49.63 Hz.

The coordinated control strategy in the over-speed power reserve area shows an obviously better frequency modulation effect than that with MPPT control, additional inertial control and variable de-loading level control. This strategy can not only provide effective inertial support, and reduce the frequency change rate at the initial stage of

**Fig. 11** Comparisons of the system variable responses when the wind speed is 8 m/s



load disturbance, but also decrease the system frequency steady-state deviation.

(2) Simulation analysis in the over-speed-pitch power reserve area

The wind speed is set to 10 m/s and the de-loading level is 6% under variable de-loading level control. In the first 5 s, the active power of the load increases by 0.4 MW, and other relevant parameters are selected as  $\Delta f_1 = 0.2\text{Hz}$ ,  $k_d = 0.4$ , and  $k_\beta = 12.5$ . Simulation tests are carried out by applying four control strategies: (1) MPPT control; (2) additional inertial control; (3) variable de-loading level control; (4) frequency coordinated control. The simulation results are indicated in Fig. 12.

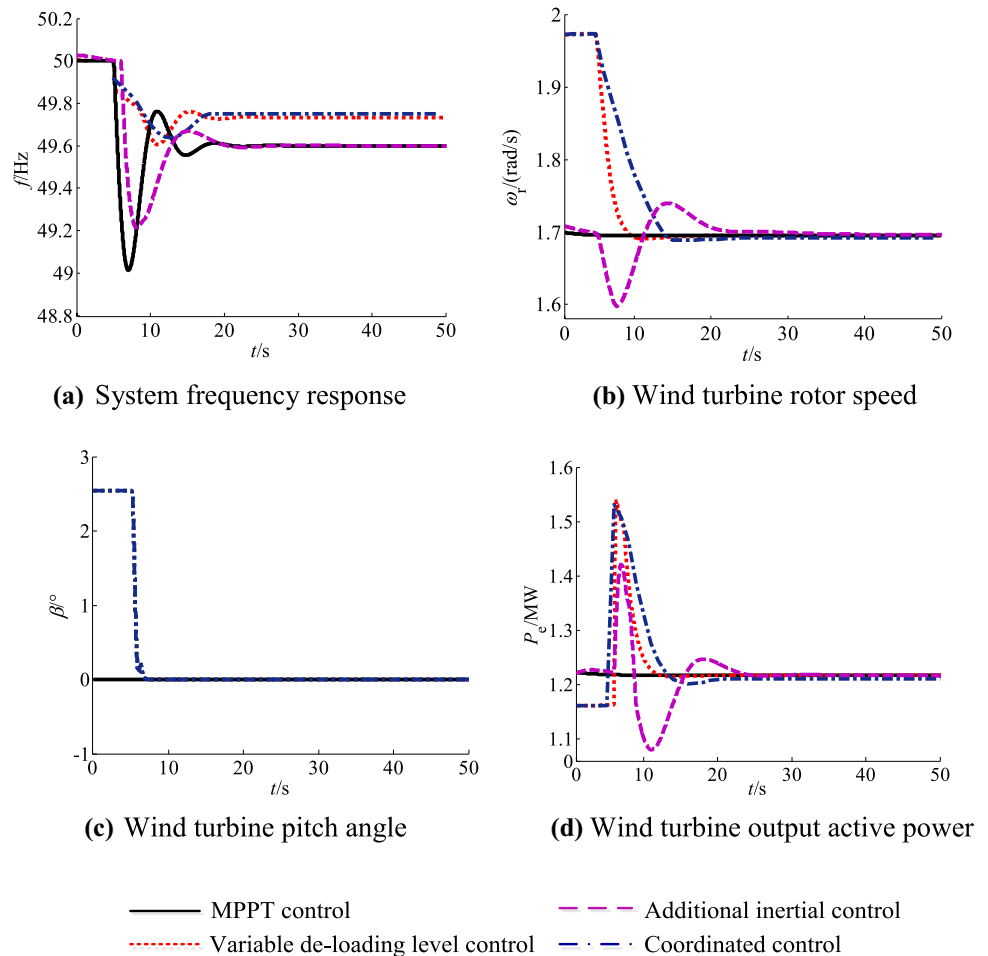
Figure 12a shows comparisons of the system frequency response after the load suddenly increases, and partial data are shown in Table 3

The D-PMSG rotor speed, pitch angle and output power remain unchanged and show almost no response to the system frequency deviation in the MPPT control mode. In the case of additional inertial control, the D-PMSG rotor speed decreases and the output active power increases under a load disturbance, which delays the system fre-

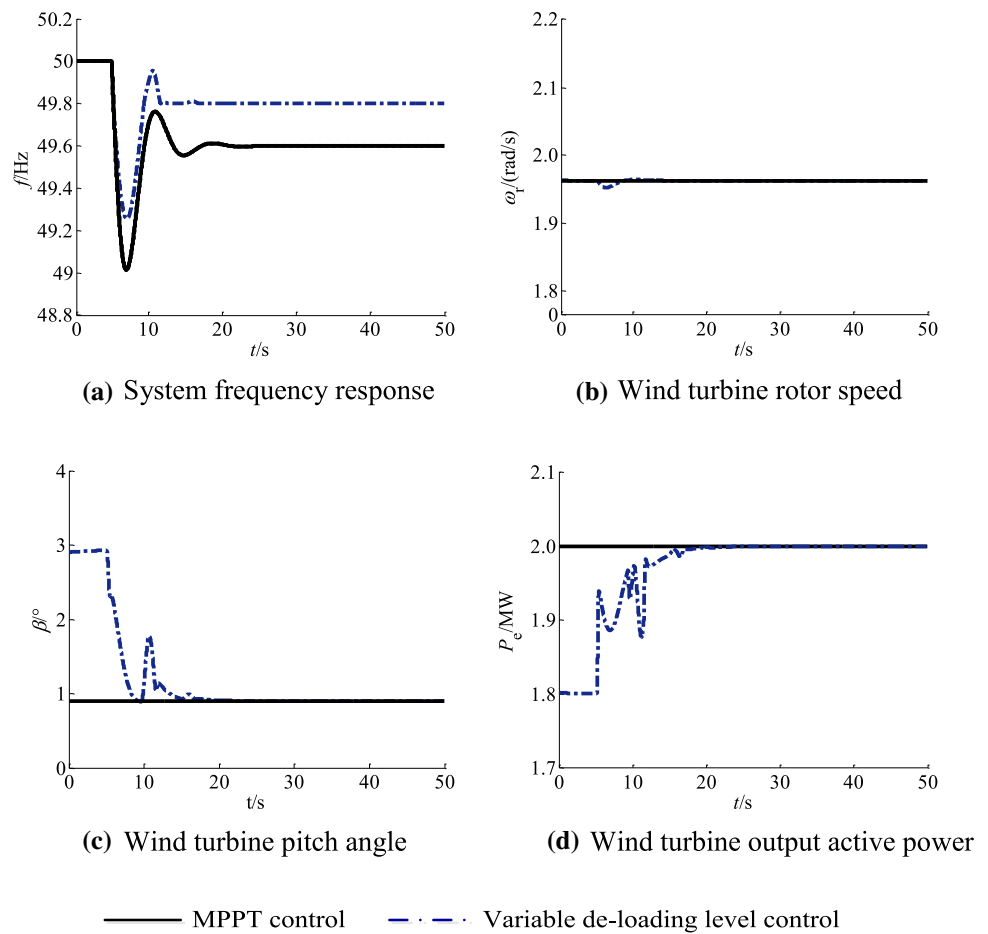
quency change. Under the variable de-loading level control mode, the system frequency change rate decreases, and the minimum value raises from 49.01 Hz to 49.60 Hz with a falling amplitude of 59%. The time to system frequency minimum value extends from 7.0 s to 10.8 s, and the steady-state value increases from 49.60 Hz to 49.73 Hz. In the case of frequency coordinated control, the system frequency minimum value raises to 49.64 Hz, the time is prolonged to 12.6 s, the frequency steady-state value increases to 49.75 Hz, and the deviation is reduced by 37.5% compared with MPPT control. It is distinct that the frequency coordinated control strategy in the over-speed-pitch power reserve area can not only reduce the frequency change rate at the initial stage of the load disturbance, but also decrease the system frequency steady-state deviation and display a significantly better frequency modulation effect.

Figure 12 (b–d) compares the dynamic responses of the rotor speed  $\omega_r$ , pitch angle  $\beta$  and output active power  $P_e$  in four cases after the load suddenly increases. In the MPPT control and additional inertial control modes, the D-PMSG retains the same rotor speed and output

**Fig. 12** Comparisons of the system variable responses when the wind speed is 10 m/s



**Fig. 13** Comparisons of the system variable responses when the wind speed is 12 m/s



**Table 2** Comparisons of the system frequency response

Control mode	$f_{min}/\text{Hz}$	$t_{min}/\text{s}$	$f_{\infty}/\text{Hz}$	$t_{\infty}/\text{s}$
MPPT control	49.01	7.0	49.60	11.3
AIC control	49.37	10.7	49.57	22.5
VD-L control	49.42	9.3	49.62	11.1
CO control	49.59	12.6	49.63	13.8

**Table 3** Comparisons of the system frequency response

Control mode	$f_{min}/\text{Hz}$	$t_{min}/\text{s}$	$f_{\infty}/\text{Hz}$	$t_{\infty}/\text{s}$
MPPT control	49.01	7.0	49.60	20.8
AIC control	49.23	10.7	49.60	22.5
VD-L control	49.60	10.8	49.73	12.9
CO control	49.64	12.6	49.75	11.5

power, and the pitch angle remains at 0° and shows little improvement in the system frequency deviation. However, in the cases of variable de-loading level control and coordinated control, the D-PMSG operates in the de-loading mode with a higher initial rotor speed and

pitch angle. As the load suddenly increases, the wind turbine rotor speed is gradually reduced to 1.7 rad/s, and the pitch angle decreases from 2.61° to 0°, which increases the active output power by 0.3 MW and delays the system frequency change. In addition, due to the role of additional inertial control, the D-PMSG rotor speed change rate is decreased, and the system frequency deviation is delayed further. Therefore, the system frequency transient response in the over-speed-pitch power reserve area is improved effectively.

(3) Simulation analysis in the pitch angle power reserve area

The wind speed is set to 12 m/s and the de-loading level is 3.5% under variable de-loading level control. In the first 5 s, the active power of the load increases by 0.4 MW. Simulation tests are carried out under the following two control strategies: (1) MPPT control; (2) variable de-loading level control. The simulation results are indicated in Fig. 13.

Figure 13a shows the comparisons of the system frequency response after the load suddenly increases, and partial data are shown in Table 4.

**Table 4** Comparisons of the system frequency response

Control mode	$f_{\min}/\text{Hz}$	$t_{\min}/\text{s}$	$f_{\infty}/\text{Hz}$	$t_{\infty}/\text{s}$
MPPT control	49.01	7.0	49.60	11.3
VD-L control	49.26	7.1	49.80	10.6

Obviously, in the case of the variable de-loading level control mode, the system frequency minimum value raises to 49.26 Hz, the time to the system frequency minimum value extends by 0.1 s, the steady-state value increases to 49.8 Hz and the system frequency setting time decreases to 10.6 s. However, the system frequency transient response is difficult to improve because of the slower pitch angle control. Due to the high wind speed, the reserved active power for frequency modulation is relatively high, so the system frequency steady-state response is significantly improved and the frequency steady-state deviation is reduced by 50% compared with MPPT control.

Figure 13 (b–d) indicate the dynamic responses of the wind turbine rotor speed  $\omega_r$ , pitch angle  $\beta$  and output active power  $P_e$  in two cases after the load suddenly increases. In the MPPT control mode, the D-PMSG operates at the optimal rotor speed and output power, which shows little improvement in the system frequency deviation. However, in the case of the variable de-loading level control mode, the D-PMSG rotor speed is almost retained at an optimal and constant value, and the initial value of the pitch angle is set as  $2.94^\circ$  to implement the de-loading operation. As the load suddenly increases, the pitch angle is gradually reduced to  $0.98^\circ$ , which makes the active output power increase by 0.2 MW. Thus, the power increment required for frequency modulation is achieved, and the system frequency steady-state deviation is reduced greatly.

## 7 Conclusions

A frequency coordinated control strategy based on the variable de-loading level for a D-PMSG wind turbine is proposed in this paper. The simplified model of the D-PMSG is established. The principle of variable de-loading level control and additional inertial control strategies are analyzed. The frequency coordinated control strategy based on the variable de-loading level is designed for different wind speed zones. Simulation results indicate that compared with traditional MPPT control, additional inertial control and variable de-loading level control, the frequency coordinated control strategy in different power reserve areas can not only provide effective inertial support for the system, but also reduce the frequency change rate at the initial stage of the load disturbance and the frequency steady-state deviation, which display a better frequency modulation capability.

**Author Contributions** Mudan LI and Yinsong WANG conceived the research; Mudan LI performed the frequency coordinated control strategy design, performed the simulation, validation, and wrote the paper; Yinsong WANG critically revised the paper and provided constructive criticism.

**Funding** This study was funded by the Joint Funds of the National Natural Science Foundation of China (grant number: U1709211); This study was funded by the Fundamental Research Funds for the Central Universities (grant number: 2020MS148).

## Compliance with Ethical Standards

**Conflicts of Interest** The authors declare that they have no conflict of interest.

## Appendix

See below Tables 5 and 6.

**Table 5** D-PMSG wind turbine parameters

Parameter	Symbol	Value
Radius of the rotor	$R$	38 m
Air density	$\rho$	1.225 kg/m <sup>3</sup>
Rated rotor speed	$\omega_n$	1.956 rad/s
Rated power	$P_n$	2 MW
Cut in wind speed	$v_{\text{cut-in}}$	3 m/s
Rated wind speed	$v_n$	11.8 m/s
Cut out wind speed	$v_{\text{cut-out}}$	25 m/s
Optimal tip speed ratio	$\lambda_{\text{opt}}$	6.3
Nominal power coefficient	$C_{\text{pmax}}$	0.438
Moment inertia constant	$J_w$	$1.5 \times 10^6 \text{ kg}\cdot\text{m}^2$
pitch servo time constant	$T_{\text{servo}}$	0.2 s
Min./Max. pitch angle	$\beta_{\text{min}}/\beta_{\text{max}}$	$0^\circ/30^\circ$
Blade pitch angle rate	$d\beta/dt_{\text{min}}/$ $d\beta/dt_{\text{max}}$	$-10^\circ/\text{s}$ $10^\circ/\text{s}$
PMSG-converter equivalent time constant	$T_A$	0.2 s

**Table 6** Speed governor, turbine and synchronous generator parameters

Parameter	Symbol	Value
PI controller gains	$k_p/k_i$	10/10
Difference coefficient	$R$	0.025
Servo inertia time constant	$T_G$	0.2 s
Turbine inertia time constant	$T_{\text{CH}}$	0.3 s
Synchronous generator inertia time constant	$H$	6 s
Synchronous generator damping coefficient	$D$	0

## References

- National Development and Reform Commission (2016) “13th Five-Year Plan” for Wind Power Development. National Energy Administration of the People’s Republic of China
- Liu ZY (2015) Global Energy Internet. China Electric Power Press
- Song HD, Dong XY (2007) Discussion on present situations and development trends of wind power generation technology. *Electrotechnics Electric* 13:1–4
- Sun YC, Liu SM, Wang ZJ et al (2016) Study of the impact of large-scale wind power access to dynamic characteristics of power system. *Syst Simul Technol* 12:83–87
- Li SH, Haskew TA, Xu L (2010) Conventional and novel control designs for direct driven PMSG wind turbines. *Electric Power Syst Res* 80:328–338
- Chinchilla M, Arnaltes S, Burgos JC (2006) Control of permanent-magnet generators applied to variable-speed wind-energy systems connected to the grid. *IEEE Trans Energy Convers* 21:130–135
- Mokadem ME, Courtecuisse V, Saudemont C et al (2009) Experimental study of variable speed wind generator contribution to primary frequency control. *Renewable Energy* 34:833–844
- Hughes FM, Anaya-Lara O, Jenkins N et al (2006) A power system stabilizer for DFIG-based wind generation. *IEEE Trans Power Syst* 21:763–772
- Conrey JF, Watson R (2008) Frequency response capability of full converter wind turbine generators in comparison to conventional generation. *IEEE Trans Power Syst* 23:649–656
- Miao ZX, Fan LL, Osborn D et al (2009) Control of DFIG-based wind generation to improve inter area oscillation damping. *IEEE Trans Energy Convers* 24:415–422
- Morren J, De Haan SWH, Kling WL et al (2006) Wind turbines emulating inertia and supporting primary frequency control. *IEEE Trans Power Syst* 21:433–434
- Kayikci M, Milanović JV (2009) Dynamic contribution of DFIG-based wind plants to system frequency disturbances. *IEEE Trans Power Syst* 24:859–867
- Erlich I, Wilch M (2010) Primary frequency control by wind turbines. In: *Proceeding of power and energy society general meeting, 2010*. IEEE, pp 1–8
- Cao ZJ (2012) Study on control strategy of DFIG wind turbine for the participation of system primary frequency regulation. Southwest Jiaotong University
- Tian XS, Wang WS, Chi YN et al (2015) variable parameter virtual inertial control based on effective energy storage of dfig-based wind turbines. *Autom Electric Power Syst* 39:20–26
- Chen YH, Wang G, Shi QM et al (2019) A new coordinated virtual inertial control strategy for wind farms. *Autom Electric Power Syst* 39:27–33
- Li HM, Zhang XY, Wang Y et al (2012) Virtual inertia control of DFIG-based wind turbines based on the optimal power tracking. *Proce CSEE* 32:32–39
- De Almeida RG, Castronuovo ED, Lopes JAP (2006) Optimum generation control in wind parks when carrying out system operator requests. *IEEE Trans Power Syst* 21:718–725
- De Almeida RG (2007) Participation of Doubly Fed Induction Wind Generators in System Frequency Regulation. *IEEE Trans Power Syst* 22:944–950
- Vidyanandan KV, Senroy N (2013) Primary frequency regulation by deloaded wind turbines using variable droop. *IEEE Trans Power Syst* 28:837–846
- Luo M (2013) Research on the variable speed variable pitch control of the large scale wind turbine. Chongqing University
- Deshpande AS, Peters RR (2012) Wind turbine controller design considerations for improved wind farm level curtailment tracking. In: *Proceedings of power & energy society general meeting*. IEEE, pp 1–6
- Jeong Y, Johnson K, Fleming P (2014) Comparison and testing of power reserve control strategies for grid-connected wind turbines. *Wind Energy* 17:343–358
- Zhang ZS, Sun YZ, Li GJ et al (2011) Frequency regulation by doubly fed induction generator wind turbines based on coordinated over-speed control and pitch control. *Autom Electric Power Syst* 35:20–25
- Li C, Li C, Kang Z et al (2014) Frequency coordinated control strategy of Variable-Speed Constant-Frequency Wind Farms in Power Grids. *Power Syst Clean Energy* 7:62–67
- Tan Y, Meegahapola L, Muttaqi KM (2016) A Suboptimal Power-point-tracking-based primary frequency response strategy for DFIGs in hybrid remote area power supply systems. *Energy conversion*. *IEEE Trans Energy Convers* 31:93–105
- Zhang GF, Yang JY, Sun F et al (2017) Primary Frequency Regulation Strategy of DFIG Based on Virtual Inertia and Frequency Droop Control. *Trans China Electrotech Soc* 32:225–232
- Zhao JJ, Lu X, Fu Y et al (2015) Dynamic Frequency Control Strategy of Wind/Photovoltaic/Diesel Microgrid Based on DFIG Virtual Inertia Control and Pitch Angle Control. *Proce CSEE* 35:3815–3822
- Ding L, Yin SY, Wang TX et al (2015) Integrated Frequency Control Strategy of DFIGs Based on Virtual Inertia and Over-Speed Control. *Power Syst Technol* 39:2385–2391
- Attya AB, Hartkopf T (2014) Wind turbine contribution in frequency drop mitigation-modified operation and estimating released supportive energy. *IET Gener Transm Distrib* 8:862–872
- Ye P, Tian RB, Teng Y et al (2015) Frequency control based on coordinated variable pitch and variable speed in DFIG. *J Shenyang Univer Technol* 3:260–267
- Jiang JL, Chao Q, Chen JW et al (2010) Simulation study on frequency response characteristic of different wind turbine. *Renewable Energy Res* 28:24–28
- Li LC, Ye L (2011) Coordinated control of frequency and rotational speed for direct drive permanent magnet synchronous generator wind speed. *Autom Electric Power Syst* 35:26–31
- Liu QH, Han XS (2014) Main steps and key technology of the simplified model for doubly-fed induction generator. *East China Electric Power* 42:0840–0845
- Auricio JM, Marano A, Gomez-Exposito A et al (2009) Frequency regulation contribution through variable-speed wind energy conversion systems. *IEEE Trans Power Syst* 24:173–180
- Eng H, Xu DW (2011) Stability analysis and improvements for variable-speed multi pole permanent magnet synchronous generator-based wind energy conversion system. *IEEE Trans Sustain Energy* 2:459–467
- Lah NR, Thiringer T, Karlsson D (2008) Temporary primary frequency control support by variable speed wind turbines potential and applications. *IEEE Trans on Power Syst* 23:601–612
- Keung PK, Li P, Banakar H et al (2009) Kinetic energy of wind turbine generators for system frequency support. *IEEE Trans Power Syst* 24:279–287

**Publisher’s Note** Springer Nature remains neutral with regard to jurisdictional claims in published maps and institutional affiliations.

**Mudan Li** was born in Shanxi, China, in 1983. She received the B.S. degree in automation, the M.S. degree in control theory and control engineering from Taiyuan University of Technology, Taiyuan, China, in 2008. She is currently a lecturer with the School of Science and Technology College, North China Electric Power University, Baoding,

China. Her research interests include clean energy power generation, advanced control theory.

**Yinsong Wang** was born in Hebei, China, in 1967. He received the B.S. degree in thermal measurement and its automation, the M.S. degree in thermal measurement and its automation, the Ph.D. degree in power

system and its automation from North China Electric Power University, Baoding, China, in 1988, 1991, and 1999, respectively. He is currently an associate professor with the School of Control and Computer Engineering, North China Electric Power University, Baoding, China. His research interests include advanced control strategy and its application in power system, performance diagnosis of control systems.